Postprint of: Linert I., Zubek M., Excited states of isoxazole molecules studied by electron energy-loss spectroscopy, Journal of Electron Spectroscopy and Related Phenomena, Vol. 243 (2020), 146981, DOI: 10.1016/j.elspec.2020.146981

Excited states of isoxazole molecules studied by electron energy-loss spectroscopy

Ireneusz Linert[1], Mariusz Zubek[1,2*]

[1]Department of Physics of Electronic Phenomena,
Faculty of Applied Physics and Mathematics,
Gdańsk University of Technology, 80-233 Gdańsk, Poland

[2]Department of Control and Power Engineering,
Faculty of Ocean Engineering and Ship Technology,
Gdańsk University of Technology, 80-233 Gdańsk, Poland

Abstract

Electron energy-loss spectra were measured in isoxazole in the excitation energy range 3.5-10 eV to investigate the valence excited states. Spectra recorded at different scattering conditions enabled the identification of the singlet and triplet states and the determination of their vertical excitation energies. The two lowest energy triplet bands, $\pi\pi^*$ $1^3A'$ and $\pi\pi^*$ $2^3A'$ at 4.20 and 5.30 eV, respectively show vibrational progressions. The first triplet state, $15a'\pi^*$ $1^3A''$ that involves excitation from the nitrogen lone-pair orbital is observed at 5.68 eV. Three singlet valence states, $\pi\pi^*$ $1^1A'$, $n_N\pi^*$ $1^1A''$ and $\pi\pi^*$ $2^1A'$ are observed at 5.96, 6.49 and 6.88 eV, respectively in accord with the absorption measurements. Resonance excitation of the triplet and singlet states was noticed.

* Corresponding author: E-mail address: marzubek@pg.edu.pl

Keywords: electronic states, isoxazole, energy-loss, excitation energy, triplet states

1. Introduction

Isoxazole belongs to a group of heterocyclic molecules that have been targets of recent spectroscopic investigations because of their wide applications in the medicinal biology and in agrochemistry. The nitrogen- and oxygen-containing heterocycles and their derivatives are exceptional components of polynucleotide strands of DNA and other cellular macromolecules. For example, the modified isoxazole ring may be discerned in double-ring purine nuclei bases, adenine and guanine. In this context, the behavior of the heterocyclic molecules in radiotherapy has been investigated, where the secondary electrons, which are produced by the primary ionizing particles, cause site-selective cleavage of the molecular bonds. Further, the bond cleavages may cause single- and double-strand breaks in the polynucleotides of DNA [1,2]. In the case of applications of the isoxazole compounds in medicine, new chemical methods for their synthesis enable the development of substances that possess diverse therapeutic applications as, for example, in anticancer, antibacterial and antidepressant drugs [3]. The isoxazole derivatives have also found application in crop protection of human activity where their insecticidal, fungicidal and herbicidal properties are exploited [4]. The recent progress in chemical and biological applications of isoxazole and its derivatives in treating various diseases, including cancer, have been recently reviewed, see [5,6] and references therein.

The isoxazole (2-azafuran) molecule, (C_3H_3NO) is a five-membered aromatic heterocycle molecule that contains one nitrogen and one oxygen heteroatom at adjacent positions in the molecular ring (Fig. 1). It is an aza-derivative of furan (C_4H_4O) and may be obtained by replacing the methine (−CH) group at position (2) or (5) in furan with a nitrogen atom. The outermost occupied orbitals in isoxazole (C_S point group) in the $\tilde{X}\,^1$A' ground electronic state are …$(15a')^2(2a'')^2(3a'')^2$, where 15a' is the σ nitrogen lone-pair n_N orbital and 2a'' and 3a'' are the π_2 and π_3 orbitals, respectively. The two lowest unoccupied (virtual) orbitals are 4a''(π_4^*) and

5a"(π_5^*). Visualization of the 3a", 2a" and 15a' orbitals, obtained from the B3LYP/6311++G(d,p) calculations [7], is shown in Fig. 2. The excitation from the highest occupied 2a", 3a" and 15a' orbitals into the two 4a" and 5a" virtual orbitals give rise to valence excited states. These consist of, four ^{1}A' and two ^{1}A" singlet states and their counterpart triplet states. Some of the states may be formed from a linear combination of these orbitals. Isoxazole is isoelectronic with furan, and therefore it may be expected that both molecules possess similar arrangements of the excited electronic bands. This similarity, however, is perturbed by excited states arising from the n_N nitrogen lone-pair orbital in isoxazole. Further, the isoxazole excited valence and Rydberg states may show vibronic coupling, which induces nonadiabatic effects. This, has been found for the low lying excited singlet states in furan [8].

The excitation spectra of the valence and Rydberg states of gas phase isoxazole have been much less frequently studied than those of furan and we can refer to the works of Walker *et al.* [9] and Cao [10]. Walker *et al.* [9] reported results of the VUV absorption and electron energy-loss measurements and of multi-reference configuration interaction (MRCI) computations. Cao [10] calculated the vertical transition energies for the first three valence singlet states at the CASPT2 level of theory. The VUV spectra measured in the energy region 5.5-10.8 eV revealed excitation of the valence and Rydberg singlet states. The first two $^1\pi\pi^*$ excited valence states appear at 6.0 and 7.0 eV and are separated by a $^1n_N\pi^*$ state at 6.5 eV. The higher $^1\pi\pi^*$ valence bands dominate the VUV spectrum in the 7.5-9.0 eV energy region with a pronounced maximum at about 8.2 eV. The Rydberg structures in the spectra correspond to the $\pi_3 n$s, $\pi_3 n$p and $\pi_3 n$d series with n = 3-7. The n = 3 first members in the $\pi_3$3s, $\pi_3$3p and $\pi_3$3d series appear at 6.801, 7.642 and 8.446 eV, respectively [9]. The electron energy-loss spectrum recorded at 100 eV is in a very good agreement with the VUV spectrum [9]. The near-threshold electron energy-loss spectra obtained using the trapped-electron spectrometer revealed the first two triplet states at 4.1

and 5.3 eV, which were assigned to $^3\pi\pi^*$ [9]. The MRCI computations aided identification of the excitation bands in the measured spectra. Recent isoxazole spectroscopic investigations include dissociative electron attachment [11], VUV threshold photoelectron [12] and photoionization and cationic fragmentation [13] studies.

The vibrational motion of the isoxazole molecule in the $\tilde{X}^1$A' electronic ground state have been studied by recording the Raman and IR spectra [14]. Eighteen normal vibrational modes of the planar isoxazole molecule are of either A' or A" symmetry and are infrared active. The totally symmetric ν_1(A')-ν_{13}(A') modes are the in-plane, while the ν_{14}(A")-ν_{18}(A") are out-of plane vibrations. The vibrational energies of the three ν_1-ν_3 C-H stretching modes are located in the 380-395 meV range, while the energies of the remaining ν_4-ν_{18} modes are lower than 200 meV [15,16].

In the present work, we report studies of the valence excited states of isoxazole molecules by applying electron energy-loss spectroscopy. This technique allows observation and differentiation between optically-allowed and more significantly optically-forbidden excitation transitions [17-19]. Here, electron scattering measurements are performed in wide ranges of electron impact energy and scattering angle. Energy-loss spectra at higher electron incident energy E_i (E_i > ~20 eV) and low scattering angle ensure the observation of the singlet states and are in good agreement with the absorption spectra. Electron scattering in the backward directions enhances the observation of the spin-forbidden states (triplet states) in the spectra, while scattering at low electron residual energy, that is at incident energy close to the excitation thresholds, increases the intensity of symmetry-forbidden excitations (also called dipole-forbidden excitations). Furthermore, the formation of negative-ion shape resonances at energies just above excitation thresholds of the states enhances their energy-loss peaks in the spectra.

We recorded electron energy-loss spectra in the excitation energy range 3.5-10 eV and at the scattering angles of 10° and 180°, aiming to obtain new data on the valence excited states of isoxazole. Of especial interest were the triplet states. Four triplet states were observed and assigned and their vertical excitation energies determined. Resonance excitation of some of the singlet and triplet states was also observed.

2. Experimental

The electron spectrometer employed in the measurements of the electron energy-loss spectra has been described in detail in our previous publications [20-22]. In outline, it consists of a source of electron beam produced by a double hemispherical selector, a capillary to form the isoxazole molecular beam and of a scattered electron analyzer that can be rotated around the axis of the molecular beam. Magnetic angle-changer [23] is placed at the collision region between the electron beam source and the scattered electron analyzer. It produces a localized magnetic field to extend the scattering angle range up to 180°. For the measurements of the threshold excitation spectra, the spectrometer was modified to apply the technique of the penetrating electrostatic field [24]. The scattered electron analyzer is also equipped with a magnetic field deflector [22] to determine the possible contribution of the low energy negative ions in the threshold electron spectra (such contribution, if present, were below 5% in the present spectra).

The electron energy-loss spectra have been measured at fixed scattering angles. Here, two modes of measurements have been applied, either the mode of the constant residual electron energy E_R or the mode of constant incident electron energy E_i. In the threshold mode, which provides energy-loss spectra for $E_R < 50$ meV, the scattered electrons were collected from a larger solid angle, up to 4π [24]. The electron energy resolution (FWHM) in the energy-loss mode was 50–80 meV. The background contribution into the measured spectra was subtracted from the recorded data. The incident electron energy was calibrated against the ^2S resonance in

helium (19.365 eV) to within ± 30 meV. The electron energy-loss was calibrated against the position of the elastic scattering peak to within ± 10 meV.

Liquid isoxazole was placed in a stainless steel container attached to a gas line. It was maintained at approximately 40°C and was degassed several times under low pressure to remove contaminating gases, nitrogen, oxygen and water vapour, before introducing into the spectrometer. Isoxazole was purchased from Sigma-Aldrich Chemie with a stated purity of 99 % .

3. Results and discussion

Selected, representative electron energy-loss spectra measured at different electron scattering conditions are shown in Fig. 3. The lower spectrum was measured at higher incident electron energy E_i = 20 eV and low scattering angle Θ = 10°, conditions which favour observation of optically-allowed transitions. The spectrum, in the general shape agrees well with the absorption measurements [9], although differs in the relative intensities of the observed bands. It displays two energy ranges, 5.5-7.5 eV and 7.5-9.5 eV of overlapping bands of the valence and Rydberg states. In the 5.5-7.5 eV energy range, we have identified three valence bands of the excitation of the singlet states (see below), in accordance with Walker et al. [9]. The broad asymmetric 7.5-9.5 eV peak acompasses excitation of the higher $^1\pi\pi^*$, $^1\pi\sigma^*$ and Rydberg states [9]. The two remaining spectra in Fig. 3, measured at lower residual electron energy, E_R = 2 and 3 eV, (that is exciting states closer to their thresholds) and a scattering angle Θ = 180°, contain, apart from the three valence singlet bands, those due to excitation of the optically-forbidden (triplet) states. This is clearly evidenced by the observation of the first triplet band at 4.20 eV, in agreement with the near-threshold electron energy-loss measurements of Walker et al [9]. Excitation of further triplet states is indicated in the E_R = 2 and 3 eV spectra by a vibrational structure at 5.3 eV and in the E_R = 2 eV spectrum by a shoulder at 5.8 eV. There is also evidence of excitation of a new band at 7.4 eV. Here, a greater energy-loss intensity is seen in the E_R = 2 and 3 eV spectra at

the minimum at 7.5 eV in comparison with the E_i = 20 eV spectrum. Excitation of the optically-forbidden states is also seen in the region of 8 eV, as marked by the shift of the maximum to lower energy (Fig. 3). Moreover, at higher energy a broad band at about 8.8 eV and an increase of intensity above 9.5 eV are also recorded in both low E_R spectra.

The 4.8-7.7 eV energy-loss range in the measured spectra is attractive for detailed analyses, since a number of singlet and triplet valence states is predicted in this region by the MRCI calculations [9]. Therefore, the 4.8-7.7 eV energy range has been analyzed in detail by using a least-square fitting routine, that is similar to the applied in our recent studies of the electronic states of pyrimidine [19], pyridine [21] and pyridazine [22]. The excitation bands were approximated by a series of introductory bi-Gaussian asymmetric profiles, which reproduce features of the spectra in the 4.8-7.7 eV energy range. The bi-Gaussian profile represents function describing each wing of the asymmetric band by its own width. Some of the bi-Gaussian profiles showed little asymmetry in the fitting and to simplify the procedure they were approximated by the Gaussian shapes. The fitting has been commenced by investigating the optically-allowed transitions. The E_i = 20 eV, $\Theta = 10^o$ spectrum was approximated by three valence bands in accord with conclusions of Walker et al. [9]. A narrow profile (0.09 eV FWHM) described excitation of the Rydberg state at 6.801 eV [9]. The spectra measured at lower E_R have been approximated by the three bands from the optically-allowed spectra and by three bands at 5.3, 5.7, and 7.4 eV, which reproduced the new features recorded in the spectra. The 5.3 eV band that shows the vibrational structure, has been composed from seven individual, narrow (0.085-0.110 eV FWHM) Gaussians, which simulate positions and intensities of the vibrational levels. The parameters of the initial profiles have been optimized to obtain simultaneously the best fits to the measured spectra (all together ten spectra). The single least-square fits have been reiterated over the measured spectra and terminated, when an acceptable agreement in all measured spectra has been

achieved. The maxima of the individual bands and their widths inferred in this procedure from the individual energy-loss spectra were within ± 50 and ± 30 meV of their average values, respectively, supporting the applied fitting routine.

Fig. 4 shows the deduced excitation bands and the final curves fitted to the selected spectra in the 4.8-7.7 eV region. The obtained vertical excitation energies taken as maxima of the bands are listed in Table 1. They are compared with those from other experimental [9] and theoretical [9,10] studies. Table 1 also contains assignments of the observed singlet and triplet states. The uncertainties in the vertical excitation energies are ± 40 meV.

The fitting procedure shows three valence singlet states having vertical excitation energies of 5.96, 6.49 and 6.88 eV. These values are in good agreement with those from the absorption measurements of Walker et al. [9] (see Table 1), who, in their MRCI calculations, identified the states as $\pi\pi^*$, $n_N\pi_4^*$ and $\pi\pi^*$, respectively. Cao [10], in his CASPT2 calculations, supported the above sequence of the three singlet states (Table 1). We clearly observe, an asymmetric shape for the $\pi\pi^*$ $1^1A'$ band at 5.96 eV (see below for further discussion of the band shape). The $n_N\pi_4^*$ $1^1A''$ band is only slightly asymmetric and has much lower intensity in comparison with the other two bands. The oscillator strength of the $n_N\pi_4^*$ $1^1A''$ state has been predicted in the MRCI calculations [9] to reach 5 % of that of the $\pi\pi^*$ $1^1A'$ state.

The lowest-lying, first, triplet state of isoxazole is seen in the spectra of Fig. 3. We determine its vertical excitation energy to be 4.20 eV and the adiabatic excitation energy to be 3.60 eV. Walker et al. [9] assigned the state to $\pi\pi^*$ $1^3A'$. We find a weak vibrational structure on the rising slope of the band, which is discerned, when a smooth curve fitted to the band is subtracted from the measured spectrum (see inset in Fig. 3 and Table 2). The energy-loss spectra measured at lower electron residual energy E_R, shown in Figs. 4b-d, are expected to reveal excitation of the triplet states lying above 5 eV. Indeed, three new bands, not seen in the E_i = 20 eV spectrum, are

recorded. We observe the second triplet state in the 5.3 eV energy region. The excitation band shows vibrational structure with the mean vibrational energy of 0.119 eV (Table 2). The vertical excitation energy is 5.30 eV and the 0-0 transition we observe at 4.95 eV. The vibrational progression shows six members. These may be tentatively assigned to the ν_{10}-ν_{12} modes responsible for ring deformation and C-C and C-O stretching vibrations [15] (see Table 2). However, in the fitting, we notice that the widths of the Gaussians reproducing the progression of the vibrational levels varied between 0.080 and 0.110 eV. The varying width may indicate appearance of more than one vibrational progression. We assign the band at 5.30 eV to excitation of the $\pi\pi^*$ 2^3A' state, which has been predicted to be at 5.457 eV in the MRCI calculations [9]. Excitation of an electron from the 2a" and 3a" C-C and C-N bonding orbitals (see Fig. 2) into the antibonding 4a" and 5a" orbitals will certainly initiate the ring stretching vibrations of the isoxazole molecule in the 2^3A' excited state. The relative intensity of the 2^3A' band in the spectra increases with increasing E_R from 0.03 (threshold excitation) to 2 eV. This behaviour indicates excitation of the 2^3A' state via a short-lived negative ion resonance, which is a core-excited shape resonance located at about 2 eV above the excitation threshold. We notice the same resonance behavior of the intensity of the 1^3A' triplet band. In the recent studies of furan, Regeta and Allan [25] observed core-excited shape resonances in the excitation of the first two triplet states of furan. Their measured excitation functions for the two triplet states showed strong, broad resonances peaking at about 3 eV above the excitation thresholds [25]. We assume an identical excitation mechanism for the two triplet states in isoxazole.

In the spectra of Figs. 4b-d an excitation band is observed at the energy of 5.68 eV. We assign it to the 15a'π^* 1^3A" triplet state, following an acceptable agreement with the calculations of Walker et al. [9], who predicted its energy at 5.897 eV. The 1^3A" state yields excitation structure between the 2^3A' triplet and the 2^1A' singlet bands. The intensity of this structure also varies with

increasing E_R, again, indicating a resonance excitation mechanism of the $1^3A''$ state. It is interesting to compare, the present E_R = 2 eV energy-loss spectrum (Fig.4c) with that measured by Regeta and Allan [25] in furan at E_R = 2.5 eV. In the energy range 5.6-5.7 eV, which corresponds to the position of the $1^3A''$ band in isoxazole spectrum, a strong minimum appears in furan. This difference between the isoxazole and furan spectra supports identification of the 5.68 eV state in isoxazole, as originating in excitation from the 15a' nitrogen lone-pair orbital. Finally, in the spectra of Figs. 4b-d we locate the next triplet band at 7.37 eV and tentatively assign it to the $15a'\pi^* 2^3A''$ configuration, which was predicted to be at 7.475 eV in the MRCI calculations [9].

The excitation band of the $1^1A'$ singlet state at 5.96 eV has dominating intensity in all the spectra of Fig. 4. Fig. 4d compares the shape of the $1^1A'$ band in the threshold spectrum with the dissociative electron attachment (DEA) band recorded around 6 eV for m/q = 50 amu (C_3N^- anion) [26] (see also Li et al. [11]). The DEA 6 eV band is superposed on a higher intensity band that has its maximum at 3.5 eV. The higher intensity background in the m/q = 50 amu spectrum has been removed for comparison. As seen in Fig. 4d, the DEA band at 6 eV has similar asymmetric shape and energy position to that of the $1^1A'$ state. A similar coincidence was observed by Regeta and Allan [25] for the $^1B_2$ energy-loss band in furan. It was suggested that the DEA shows evidence for the formation of "threshold resonance where the incoming electron is temporarily captured in a diffuse orbital around a valence excited core" [25]. A similar resonance excitation mechanism may exist for the $1^1A'$ state in isoxazole.

4. Conclusions

The electron energy-loss spectra were measured at different scattering conditions to investigate the valence excited states of isoxazole. The magnetic angle-changing technique was used to record backward scattering at the angle of 180°. The varied scattering conditions for the

energy-loss measurements enabled the observation of the singlet and triplet states. The energy-loss spectra were examined by using iteration fitting routine to reveal the vibronic excitation bands. In the obtained spectra, we identified excitation of four triplet states and determined their vertical excitation energies. The two lowest energy $\pi\pi^*$ $1^3A'$ and $\pi\pi^*$ $2^3A'$ triplet bands, which we found at 4.20 and 5.30 eV, respectively, show structures of vibrational progressions. The vibrational progressions correspond to modes of ring deformation and C-C and C-O stretching vibrations. We find the $15a'\pi^*$ $1^3A''$ state, the first triplet state originating in excitation from the nitrogen lone-pair orbital, at 5.68 eV. A comparison of the excitation band of the $1^1A'$ state at 5.96 eV with the dissociative electron attachment band at 6 eV indicates formation of a threshold resonance in the excitation, where an incoming electron is bound in a diffuse orbital to the $1^1A'$ excited state. Such excitation resonance mechanism is common in many organic compounds [25]. The MRCI calculations of Walker et al. [9] are in fair agreement with our vertical excitation energies.

Acknowledgements

We are grateful to Dr Iwona Dąbkowska for calculating molecular orbitals of isoxazole. This work was carried out within COST Action "Electron Controlled Chemical Lithography".

References

[1] M.A. Huels, B. Boudaïffa, P. Cloutier, D. Hunting, L. Sanche, J. Am. Chem. Soc. 125 (2003) 4467.

[2] Y. Zheng, L. Sanche, Int. J. Mol. Sci. 20 (2019) 3749.

[3] G.N. Pairas,F. Perperopoulou, P.G. Tsoungas, G. Varvounis, ChemMedChem 12 (2017) 408.

[4] C. Lamberth, J. Heterocyclic Chem. 55 (2018) 2035.

[5] N. Agrawal, P. Mishra, Med. Chem. Res. 27 (2018) 1309.

[6] J. Zhu, J. Mo, H. Lin, Y. Chen. H. Sun, Bioorg. Med. Chem. 26 (2018) 3065.

[7] M. Zubek, T.J. Wasowicz, I. Dąbkowska, A. Kivimäki, M. Coreno, J. Chem. Phys. 141 (2014) 064301.

[8] E.V. Gromov, A.B. Trofimov, N.M. Vitkovskaja, H. Köppel, J. Schirmer, H.-D. Meyer, L.S. Cederbaum, J. Chem. Phys. 121 (2004) 4585.

[9] I.C. Walker, M.H. Palmer, J. Delwiche, S.V. Hoffmann, P. Limão-Vieira, N.J. Mason, M.F. Guest, M-J. Hubin-Franskin, J. Heinesch, A. Giuliani, Chem. Phys. 297 (2004) 289.

[10] J. Cao, J. Chem. Phys. 142 (2015) 244302.

[11] Z. Li, I. Carmichael, S. Ptasińska, Phys. Chem. Chem. Phys. 20 (2018) 18271.

[12] M. Dampc, B. Mielewska, M.R.F. Siggel-King, G.C. King, B. Sivaraman, S. Ptasińska, N.J. Mason, M. Zubek, Chem. Phys. 367 (2010) 75.

[13] T.J. Wasowicz, A. Kivimäki, D. Catone, R. Richter, Int. J. Mass Spectrom. 449 (2020) 116276.

[14] F. Hegelund, R.W. Larsen, F.M. Nicolaisen, M.H. Palmer, J. Mol. Spectrosc. 229 (2005) 244.

[15] A.A. El-Azhary, H.U. Suter, J. Phys. Chem. 99 (1995) 12751.

[16] E.G. Robertson, J. Mol. Spectrosc. 231 (2005) 50.

[17] S. Trajmar, J.K. Rice, A. Kuppermann, Adv. Chem. Phys. 18 (1970) 15.

[18] M. Allan, J. Electron. Spectrosc. Rel. Phenom. 48 (1989) 219.

[19] I. Linert, M. Zubek, Chem. Phys. Lett. 624 (2015) 1.

[20] I. Linert, M. Zubek, J. Phys. B: At. Mol. Opt. Phys. 39 (2006) 4087.

[21] I. Linert, M. Zubek, Eur. Phys. J. D 70 (2016) 74.

[22] I. Linert, M. Zubek, J. Electr. Spectrosc. Rel. Phenom. 233 (2019) 69.

[23] I. Linert, G.C. King, M. Zubek, J. Electr. Spectrosc. Rel. Phenom. 134 (2004) 1.

[24] M. Zubek, M. Dampc, I. Linert, T. Neumann, J. Chem. Phys. 135 (2011) 134317.

[25] K. Regeta, M. Allan, Phys. Rev. A 91 (2015) 012707.

[26] M. Dampc, M. Zubek, unpublished results.

Figure captions

Fig. 1. Diagrams of the isoxazole and furan molecules.

Fig. 2. Visualization of the three highest occupied 3a", 2a" and 15a' molecular orbitals of isoxazole [7].

Fig. 3. Electron energy-loss spectra measured in isoxazole at: E_R = 2 eV and Θ = 180º, E_R = 3 eV and Θ = 180º and E_i = 20 eV and Θ = 10º. The structures in the spectra corresponding to the Rydberg states are indicated by R. The vertical dashed lines evidence shifts of the peaks in the spectra. The inset shows a weak vibrational structure on the rising slope of the first band in the E_R = 2 eV and Θ = 180º spectrum. The vibrational structure was obtained as a difference of the measured spectrum and a smooth curve fitted to the band.

Fig. 4. The 4.8-7.7 eV energy region of the electron energy-loss spectra measured in isoxazole at: (a) E_i = 20 eV, Θ = 10º , (b) E_R = 3 eV, Θ = 180º , (c) E_R = 2 eV, Θ = 180º , (d) E_R = 0.03 eV (threshold spectrum). Excitation bands fitted to the experimental spectra and their final fits are shown by the full lines. In (d) the 6 eV dissociative electron attachment (DEA) band [26] is shown by the dash-dot line.

Table 1. Vertical excitation energies (in electron volts) of the electronic states of isoxazole.

Assignment		Experiment			Calculations	
		Present work	UV [9]	EEL [9]	MRCI [9]	CASPT2 [10]
singlet states						
$\pi \rightarrow \pi^*$	$1^1A'$	5.96	5.96	6.0	6.298	6.34
$n_N \rightarrow \pi^*$	$1^1A''$	6.49	6.4	6.6	6.531	6.77
$\pi \rightarrow \pi^*$	$2^1A'$	6.88	6.96		6.990	7.46
$\pi_3 \rightarrow 3p$		7.65	7.642		7.523	
triplet states						
$\pi \rightarrow \pi^*$	$1^3A'$	4.20		4.1	4.060	
$\pi \rightarrow \pi^*$	$2^3A'$	5.30		5.2	5.457	
$n_N \rightarrow \pi^*$	$1^3A''$	5.68			5.897	
$n_N \rightarrow \pi^*$	$2^3A''$	7.37			7.475	

Table 2. Energies (in electron volts) of the vibrational levels in the $1^3A'$ and $2^3A'$ triplet bands. Vibrational energies are calculated as differences between energies of the vibrational levels. Comparison is made with selected modes of the $\tilde{X}\,^1A'$ ground state of isoxazole.

Energy	Vibrational energy					
$1^3A'$		$2^3A'$		$\tilde{X}\,^1A'$ [a]		
				Mode		Description
3.60		4.95				
	0.123		0.115	ν_{12}	0.112	ring deformation
3.723		5.064				
	0.115		0.116	ν_{11}	0.114	ring deformation
3.838		5.180				
	0.109		0.122	ν_{10}	0.127	C-C, C-O stretching CH rocking
3.947		5.302				
			0.123			
		5.425				
			0.118			
		5.543				

[a] selected vibrational modes of the $\tilde{X}\,^1A'$ ground state of isoxazole [16].

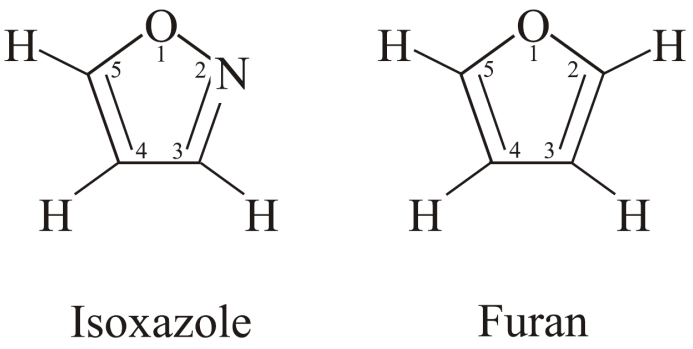

Isoxazole Furan

Fig. 1

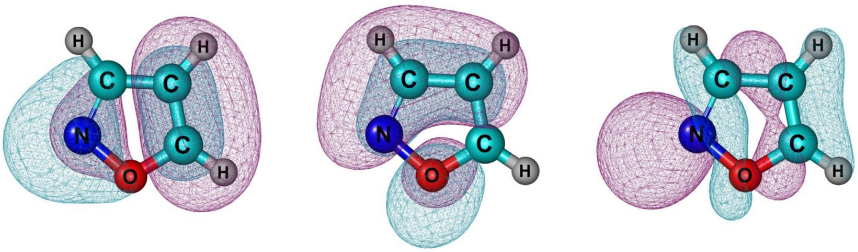

Fig. 2

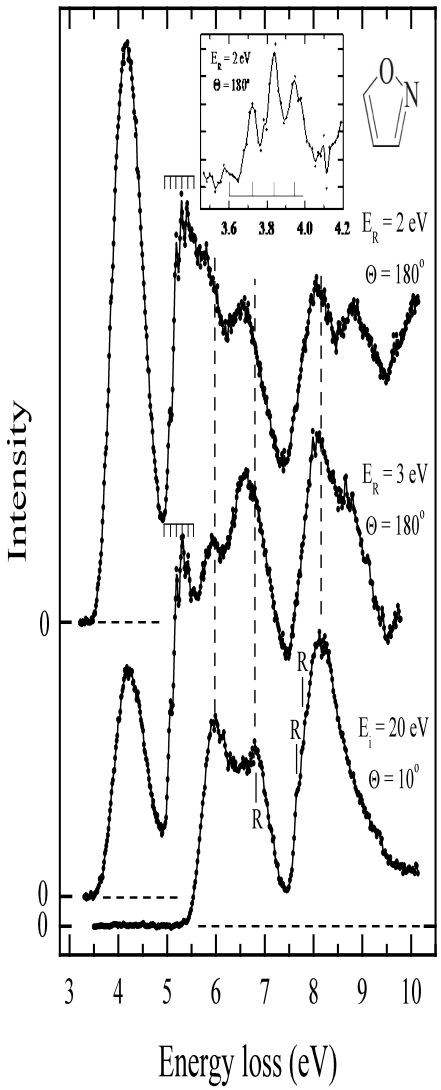

Fig. 3

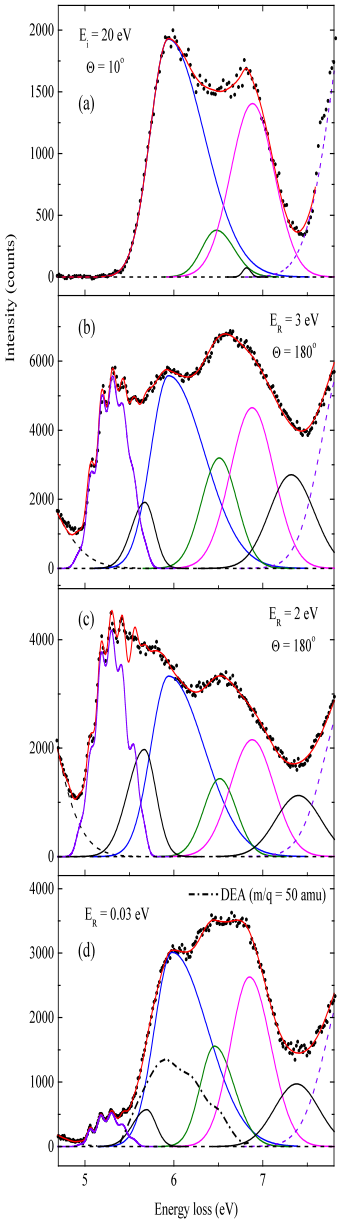

Fig. 4